Models for Nociception Stimulation and Memory Effects in Awake and Aware Healthy Individuals

Dana Copot, *Member, IEEE*, and Clara Ionescu, *Member, IEEE*

Abstract*—*Objective: **This paper introduces a primer in the health care practice, namely a mathematical model and methodology for detecting and analysing nociceptor stimulation followed by related tissue memory effects. *Methods:* Noninvasive nociceptor stimulus protocol and prototype device for measuring bioimpedance is provided. Various time instants, sensor location, and stimulus train have been analysed. *Results:* The method and model indicate that nociceptor stimulation perceived as pain in awake healthy volunteers is noninvasively detected. The existence of a memory effect is proven from data. Sensor location had minimal effect on detection level, while day-to-day variability was observed without being significant. *Conclusion:* Following the experimental study, the model enables a comprehensive management of chronic pain patients, and possibly other analgesia, or pain related regulatory loops. *Significance:* A device and methodology for noninvasive for detecting nociception stimulation have been developed. The proposed method and models have been validated on healthy volunteers.**

***Index Terms*—Nociceptor pathway, chronic pain, analgesia, bioimpedance, fractional order impedance models, non-invasive measurement, mathematical model.**

I. Introduction

PAIN is a very subjective and personal sensation, especially in awake and aware individuals [1], [2]. The self-evaluation metrics often become biased by the tissue memory, i.e., perception of pain in its absence, or artificially elevated levels of pain due to anxiety, dis-comfort and fear [3].

According to the National Institute for Health (NIH), patient self- reporting is the *most reliable indicator of the existence and intensity of pain* [4]. Subjective pain measures that may need to be quantified include intensity, time course, quality, impact, and personal experience. To that end, unidimensional pain scales have been developed. Because of their ease of use, these scales have become popular tools used to quantify pain relief and pain intensity. The most frequently used tools to assess acute pain are the numeric rating scale (NRS) and the visual analogue scale (VAS), ranging from 0 (no pain) to 10 (excessive pain). However, many critically ill patients are unable to communicate effectively because of cognitive impairment, sedation, paralysis, or mechanical ventilation. Another group unable to communicate pain are neonates and infants [5]. As such, no single tool is universally accepted for use in the non-communicative (anesthetized) patient [6], [7]. When a patient cannot express himself, observable indicators - both physiologic and behavioral - have been treated as pain-related indicators to evaluate pain level [8]. Thus the numbers are simply estimates of the perception of the pain, based on past personal experience. Quantification of the experience requires the individual to abstract and quantify the sensation. The use of unidimensional pain scales is more appropriate in the setting of acute pain (caused by surgery, broken bone, burns, etc.) than chronic pain (e.g., headache, cancer pain, low back pain, etc.). Chronic pain is usually associated with other events such as degree of support and depression. The assessment of chronic pain often requires more complex evaluation tools.

For patients in general anesthesia or intensive care unit (ICU), there is no objective or analytical tool to evaluate the level of pain they are experiencing [9]. It has been reported that 35% to 55% of nurses underrate patients pain [10], [11]. Moreover, in [12] has been reported that 64% of the patients did not receive any medications before or during painful procedures. In the SUPPORT (Study to Understand Prognoses and Preferences for Outcomes and Risks of Treatment) report [13], nearly 50% of patients reported pain, 15% reported moderately or extremely severe pain that occurred at least half of the time of the procedure, and nearly 15% were dissatisfied with their pain control. Inaccurate pain assessment and the resulting inadequate treatment of pain in critically ill adults can have significant physiologic consequences [14].

On the other hand, effective management of analgesia in the ICU units requires an assessment of the needs of the patient, subjective and/or objective measurement of the key variables (such as pain, agitation, and level of consciousness), and titration of therapy to achieve specific targets [6], [15], [16]. It is important to admit that patient needs can differ depending on clinical circumstances, and that for any given patient therapeutic targets are likely to change over time, mainly due to drug trapping [17]. Thus, achieving patient comfort and ensuring patient safety, including avoidance of over- and under-dosage, relies on

Manuscript received January 30, 2018; revised May 14, 2018; accepted June 30, 2018. Date of publication July 13, 2018; date of current version February 18, 2019. This work was supported by the Flanders Research Center under Grants G026514N and G008113N. The work of C. Ionescu was supported by the Postdoctoral Fellowship under Grant 12B3415N. *(Corresponding author: Dana Copot.)*

D. Copot is with the Research Group of Dynamical Systems and Control, Ghent University, Ghent 9000, Belgium and also with the Core Lab EEDT, Flanders Make, Lommel 3920, Belgium (e-mail: dana.copot@ugent.be).

C. Ionescu is with the Research group of Dynamical Systems and Control, Ghent University and also with the Core Lab EEDT, Flanders Make and Department of Automatic Control, Technical University of Cluj-Napoca.

Digital Object Identifier 10.1109/TBME.2018.2854917

TABLE I
BIOMETRIC DATA OF VOLUNTEERS

Index	Age	BMI	Gender
1	38	32	F
2	35	29	M
3	33	22	F
4	31	30	M
5	30	26	M
6	28	21	F
7	27	27	M

BMI given as rounded value.

TABLE II
THE TIME INTERVALS AND ACTIONS WITHIN THE 10 MINUTE MEASUREMENT PROTOCOL

Time Interval (min)	Nociceptor stimulation
0-2	Absent (NP)
2-3	Present (P)
3-6	Absent (NP)
6-7	Present (P)
7-10	Absent (NP)

The P/NP denote the acronym used in figures to indicate the case.

accurately measuring pain, agitation, sedation, and other related variables. This should be evaluated with validated tools that are easy to use, precise, accurate, and sufficiently robust to include a wide range of behaviors. From the point view of analgesia management, there is still missing an objective pain measurement tool. A comprehensive review of available tools to extrapolate on pain levels is given in [18].

Studies reporting effective pain assessment using time-frequency wavelet representation use EEG signal to extract information [19], [20]. This is indeed suitable for chronic pain subjects, but may not be applicable for general anesthesia. Hypnosis, an element of general anesthesia, is measured using EEG on the forefront of the patient, e.g., give by Bispectral Index. In this context, the pain measurement also based on EEG signal may be biased by the effects on the EEG of hypnotic agents such as Propofol.

Accordingly, the present study aims to 1) provide a method and protocol for detecting nociceptor stimulation and 2) analyse the variability in perception of pain in awake and aware individuals. This work is based on a validated lumped parameter model (LPM), often referred as fractional order impedance model for biological tissues [37]. The methods detail the model components and the necessary changes for this study compared to previous work. The results are compared to the clinical literature, taking into account the scarcity of similar data.

II. MATERIALS AND METHODS

A. Volunteers

The above described case studies have been investigated on a group of 10 volunteers. The biometric parameters are given in Table I.

All subjects provided written informed consent before participating in the study.

B. Measurement Protocol

Three study cases have been analysed:

- case 1 - perform two consecutive measurement protocols to investigate the repeatability and existence of pain memory. Sensors are placed on the right hand and the nociceptor stimulation is applied at the same location (i.e., same hand);
- case 2 - perform only one measurement as in case 1, but on a consecutive day (same hour during the day) - to test day-to-day variability in the data;
- case 3 - perform one measurement to investigate whether the sensor placement influences the measured result, i.e., the electrodes are placed on the right hand palm, while the nociceptor stimulation is applied on the left hand.

In each case, the protocol summarized in Table II has been applied.

C. Methodology

There is an established relation between nociceptor pathway and dynamics of potassium channels, i.e., the sodium-potassium pump, for signalling among intra- and extra-cellular fluid in the biological tissue [22]. Potassium is one of the most common cation in the body and the principal intracellular cation. Approximately 3500 mmol of potassium are present in the body. The distribution of Na^+ and K^+ can be thought of as opposite: one is in high concentration and the other is at low concentration. Sodium is the most prevalent cation in the extracellular fluid (ECF), with a normal level of around 140 mmol/L, but has a typical intracellular concentration of around 10 mmol/L. In contrast, potassium is the most prevalent cation in the intracellular uid, with a concentration around 150 mmol/L and about 5 mmol/L in the ECF [23]. Because the intracellular space is the largest fluid compartment in the body, this makes it the most abundant cation overall. Hence, Na^+ and K^+ can only cross where specific carrier proteins allow them to do so. Excitable cells can change their permeability to allow the in flux and efflux of ions that constitute an action potential. At rest, the large concentration gradients for Na^+ and K^+ are maintained by the action of Na^+/K^+ pump [23]. This also maintains the net negative resting membrane potential, since it involves a net transfer of one positive charge out of the cell on each cycle [24], [25]. The observed increase in potassium concentration in the ECF varies between 0.1 and 10.0 mmol/L and depends on stimulation frequency, intensity, and duration [26]. In vitro validation studies have been performed to verify the use of the proposed models for detecting changes in the concentration of these cations in controlled environment solutions [27].

From this initial step, we extrapolated that one may measure non-invasively the changes in the signalling pathways by means of bio-electrical-impedance, via the skin [28]. The proposed method for measurement is based on sending an excitatory electrical signal to the skin, while measuring its response as voltage and current changes. By changing the signalling conditions (i.e., with mechanical nociceptor stimulation) the impedance so measured changes its values as well, hence by the movement of the

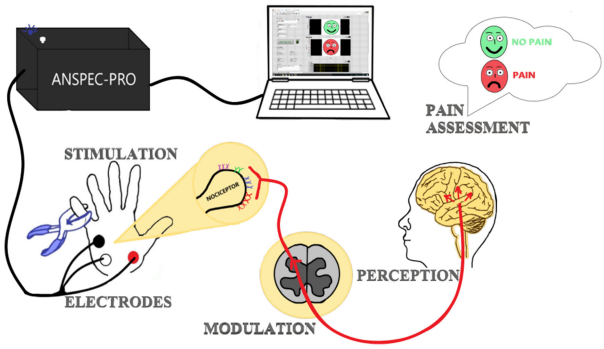

Fig. 1. The ANSPEC-PRO prototype for non-invasive measurement of bio-electrical skin impedance.

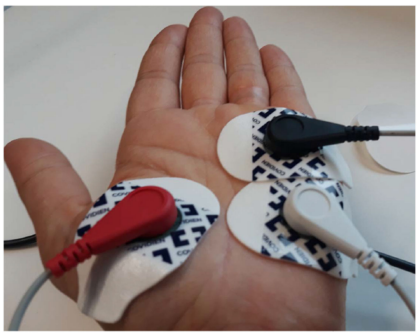

Fig. 2. Placement of the electrodes during proof-of-concept measurements; two current-carrying (CC) electrodes (white, red) and one pick-up (PU) electrode (black).

cations as a result of changes in the intra- and extra-cellular fluid composition.

For this purpose, a prototype device has been developed, ANSPEC-PRO, depicted in Figure 1.

The measurement flowchart can be summarized as follows:

- make a multisine signal with 29 components in the frequency interval 100–1500 Hz, with step interval of 50 Hz
- send this signal and acquire the measured signals at sampling frequency of 15 KHz
- the multisine signal is send with an amplitude of 0.2 mA, still a factor 5 below the maximum allowed by clinical standards [29].
- use a 3M 3-point electrode sensor in the hand-palm CE-marked (according to MDD93/42/EEC)
- measure current and voltage via a National Instruments (Texas, USA) device (cRIO9074 with NI9201- and NI9263-slots)
- store the signals online in computer for further processing.

The computer is a laptop with the operating system Windows 7 Enterprise 64-bit and a INTEL(R) Core(TM) i7-6600U CPU@2.80 GHz processor. A graphical user interface allows monitoring of signal quality.

The measurement requires three-point electrodes: two current-carrying electrodes and one pick-up electrode. The latter is measuring the voltage without carrying any currents, hence, no polarization occurs. All electrodes were placed on the palmar side of the hand (see Figure 2). A calibration of the measurements was performed for each volunteer by measuring for 10 minutes without nociceptor stimulus applied and without removing the electrodes.

D. Mathematical Models

1) Signal Processing: The measured signals are filtered for noise prior to apply non-parametric identification methods [30]. Given the input is of sinusoidal type ($A\sin(\omega t)$), the impedance is a frequency dependent complex variable evaluated as:

$$Z(j\omega) = \frac{S_{XX}(j\omega)}{S_{XY}(j\omega)} \tag{1}$$

where $S_{XX}(j\omega)$ denotes the auto-correlation spectrum of the signal, $S_{XY}(j\omega)$ denotes the cross-correlation spectra between the input-output signals, $\omega = 2\pi f$ is the angular frequency in rad/s, with f the frequency in Hz, and $j = \sqrt{-1}$. Classical periodogram filtering technique has been applied with no overlapping interval, with windowing function Blackman implemented in Matlab environment [30]. The impedance is then evaluated every minute from online data streaming and plotted against frequency. This is then a frequency response either in complex form (Real and Imaginary Parts), either in Bode plot form (Magnitude and Phase).

2) Parametric Model in Zero-Pole Form: From the frequency response determined apriori, one is able to identify a parametric model in the form of a rational function in the complex variable $s = \sigma + j\omega$, that is:

$$H(s) = \frac{b_m s^m + b_m s^{m-1} + \cdots + b_1 s + b_0}{a_n s^n + a_{n-1} s^{n-1} + \cdots + a_1 s + a_0} \tag{2}$$

with m and n the coefficient number and b and a polynomials. Often, these polynomials are factorized in zero-pole form:

$$H(s) = K\frac{(s-z_1)(s-z_2)\ldots(s-z_{m-1})(s-z_m)}{(s-p_1)(s-p_2)\ldots(s-p_{n-1})(s-p_n)} \tag{3}$$

As written in (3) the z_i's are the roots of the numerator and are defined to be the system $zeros$. The p_i's are the roots of the denominator and are defined to be the system $poles$. These models may have real, complex conjugate or combinations of such zero-pole pairs.

3) Fractional Order Model Impedance: Originating our prior work on modelling biological tissue with fractional order impedance models (FOIMs), the following extension is proposed.

The physiological pathway of pain can be described to four main processes [22]:

- transduction - when a stimulus is applied to the skin, the nociceptors located there trigger action potentials by converting the physical energy from a noxious thermal, mechanical or chemical stimulus into electrochemical energy,
- transmission - the signals are subsequently transmitted in the form of action potentials (similar to pulse trains) via nerve fibers from the site of transduction (periphery) to the dorsal root ganglion, which then activates the interneuron,
- perception - the appreciation of signals arriving in specified areas in the cerebral cortex as pain, and

- modulation - descending inhibitor and facilitator input from the brainstem that influences (modulates) nociceptive transmission from the spinal cord.

The stimulus effect to nociception reception is essentially considered an ultra-capacitor, which is represented by a non-rational form of transfer function model in $(j\omega)^n$, with n any real number [31], [32]. Specifically, skin -electrode interface, stratum corneum and ionic pathways can be modelled as elements in an electrical network. Various models describe this interface using constant or current-depending resistive-capacitive equivalent circuits [33]–[36]. Using fraction expansion theory, a lumped FOIM can be obtained as a fractional order integral [21]. Similarly, *transmission* in signalling pathways occurs via neuronal activity, already modelled with FOIMs from resistance - inductance equivalent electrical network elements [38], expressed by a fractional order derivative.

The perception model based on exponential and power law combined functions seems to be a good candidate for capturing essential electrical activity modulated in brain [39]. Plasticity in synaptic variance is introduced in a layer-based sensory area in cortex by reverse node engineering modelling [40]. In the case of pain perception, the combined effect can be obtained by using the Mittag-Leffler function, which is well-known to capture hybrid exponential and power-law behaviour in biological tissues [41], [42].

Diffusion of perception sensory activity in brain using Mittag Leffler function in time domain corresponds to a non-integer order derivative easily expressed in frequency domain [43]. Layered activity can be represented by ladder networks with serial connection of RC-cells. To account for plasticity, the RC cells are not identical, instead they behave as a memristor with unbalanced dynamics. For instance, it is expected that the first pain perception is more intense than the second, given the latency of the delayed pain stimulus (i.e., sharp first increase followed by slowly decaying tail).

Assuming the brain-cortex area as a porous tissue whose porosity varies (i.e., intra- and extra- cellular space tissue with different densities), one can model the changes in viscosity as a function of this porous density. It has been shown that fractional order derivatives are natural solutions to anomalous diffusion equations [37], [41], [43], [44]. The use and physical interpretation of this very useful fractional calculus tool has been discussed in several works, e.g., [41], [45]–[48]. The net advantage of using the Mittag-Lefler function is that it allows introducing memory formalism [49], therefore taking into account the tissue rheology. The mixed area in brain tissue will introduce a dynamic viscosity and thus a dynamic perception of nociceptor induced pain [50], [51]. Finally, the perception and modulation activity can be characterized yet again by a FOIM as differ-integral (depending on the sign of the non-rational order) [43], [52].

The complete lumped FOIM model is then given by the following terms:

$$Z_{FOIM}(s) = R + \frac{TD}{s_1^{\alpha}} + \frac{TS}{s_2^{\alpha}} + Ps_3^{\alpha} \tag{4}$$

where $\alpha_1, \alpha_2, \alpha_3 \in (-1, 0) \cup (0, 1)$ and TD-denotes transduction, TS denotes transmission and P denotes perception. A calibration factor has been added, a gain R. It may be that not all terms in this model are necessary at all times, as some of the physiological processes may be impaired in some applications (e.g., analgesia will put zero the effect of the perception term in P) [53]. The units are arbitrary, as the model is defined as a difference to the initial state of the patient - due to the use of fractional derivatives - and not as absolute values. This enables patient specificity since no generic model is assumed to be valid and thus broadcasts a new light upon the interpretation of such models.

E. Statistical Analysis

One way `anova` has been used to compare among the group of values. The function `anova1` has been used in Matlab which returns box plots of the observations in data y, by group. Box plots provide a visual comparison of the group location parameters. If y is a vector, then the plot shows one box for each value of group. If y is a matrix then the plot shows one box for each column of y. On each box, the central mark is the median and the edges of the box are the 25th and 75th percentiles (1st and 3rd quantiles). The whiskers extend to the most extreme data points that are not considered outliers. The outliers are plotted individually. The interval endpoints are the extremes of the notches. The extremes correspond to

$$\frac{q2 \pm 1.57(q3 - q1)}{\sqrt{n}} \tag{5}$$

where $q2$ is the median (50th percentile), $q1$ and $q3$ are the 25th and 75th percentiles, respectively, and n is the number of observations (excludes NaN values).

Confidence intervals have been calculated at 95%, and significant differences defined for $p - values < 0.05$. The function `ttest` in Matlab has been used.

A multiple comparison test has also been performed, using `multcompare` command in Matlab. Each group mean is represented by a symbol, and the interval is represented by a line extending out from the symbol. Two group means are significantly different if their intervals are disjoint; they are not significantly different if their intervals overlap. The input is a structure `stats` as a result of the `anova1` test. Two medians are significantly different at the 5% significance level if their intervals do not overlap.

III. Results and Discussion

A. Frequency Response Complex Impedance

The frequency response of the complex impedance calculated using (1) is depicted in Figure 3 for one individual test. In this figure one may observe the following:

- applying the same mechanical nociceptor stimuli, the real part of the impedance decreases from P1 to P2 - i.e., the level of perception of the pain is lower

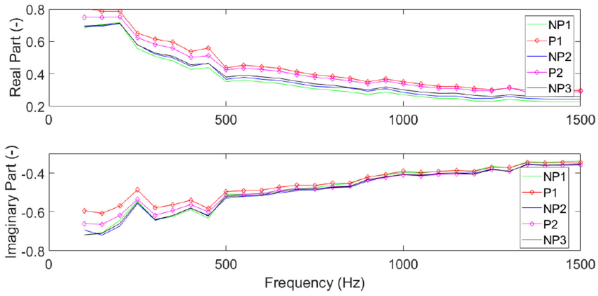

Fig. 3. Normalized impedance as a function of frequency by means of its real and imaginary parts, calculated per interval of absent(NP)/present(P) nociceptor stimulation.

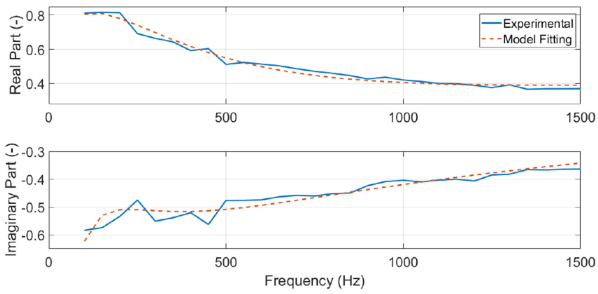

Fig. 4. Identified transfer function model for the data P1 depicted in Figure 3.

- the impedance values during absence of nociceptor stimulation increases from one interval NP1 to another, NP2, NP3 - i.e., the memory of the stimulation persists in the tissue.

The self-evaluation based on the Wong-Baker scale was between 2–3. This self-evaluation was present in all individuals during the measurements, always ranging between 2–4.

B. Transfer Function Model

For the same individual, for the pain interval, the fitting of the transfer function model from (3) onto the frequency response complex impedance data is depicted in Figure 4. The fitting was obtained using nonlinear least squares identification, with steepest gradient descent, in an iterative manner. Iteration was performed as to avoid local minimum and the number of iterations between the identified results varied between #2–#4 in all data. The iteration was stopped when the model parameters changed less that 5%.

C. FOIM Model

For the same individual, for the pain P1 interval, the fitting of the FOIM model from (4) onto the frequency response complex impedance data is depicted in Figure 5. The fitting was again obtained using nonlinear least squares identification, with steepest gradient descent, in an iterative manner. Iteration was performed as to avoid local minimum and the number of iterations between the identified results varied between #2–#4 in all data. The iteration was stopped when the model parameters changed less that 5%.

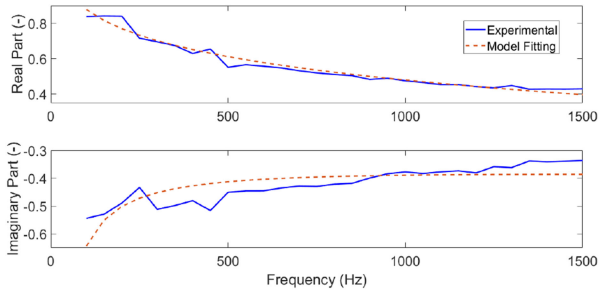

Fig. 5. Identified FOIM model for the data P1 depicted in Figure 3.

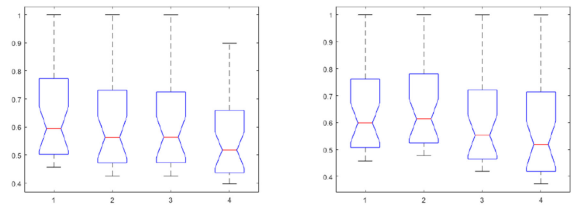

Fig. 6. Anova analysis of absolute values of frequency response complex impedance in one individual per protocol. Group 1 and Group 2 belong to case study #1, namely the two consecutive measurements. Group 3 and Group 4 denote the case study #2 and #3, respectively. Figure on left for P1 stimulation time interval, figure on right for P2 stimulation time interval.

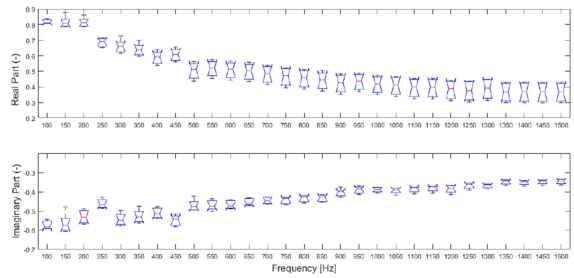

Fig. 7. Boxplot analysis of frequency response complex impedance in all individuals in study case 1, first measurement, first nociceptor stimulation (P1).

D. Variability Within Individual

To analyse the variability within individual among the three study cases, the frequency response obtained using (1) has been used. For this analysis, the absolute values of the frequency response complex impedance per excited frequency point has been used.

There was no difference within individual per protocol in either nociceptor stimulation case P1 ($p < 0.311$) or P2 ($p < 0.28$). See Figure 6.

E. Variability Among Individuals

The variability among individuals has been analysed in the frequency response of the complex impedance for the study case 1, for the first measurement, in terms of the first P1 and second P2 nociceptor stimulation. The results by means of boxplot are depicted in Figure 7 and 8, respectively. There was no significant difference among the two nociceptor stimulation time stamps, except in one individual. This however, is an individual with

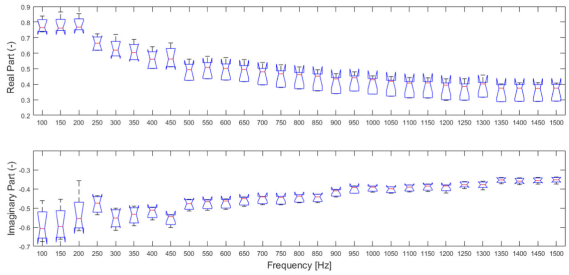

Fig. 8. Boxplot analysis of frequency response complex impedance in all individuals in study case 1, first measurement, second nociceptor stimulation (P2).

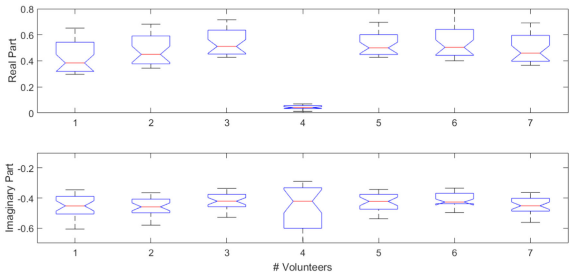

Fig. 9. Boxplot analysis of the absolute values of the frequency response complex impedance in all individuals in study case 1, first measurement, first nociceptor stimulation (P1).

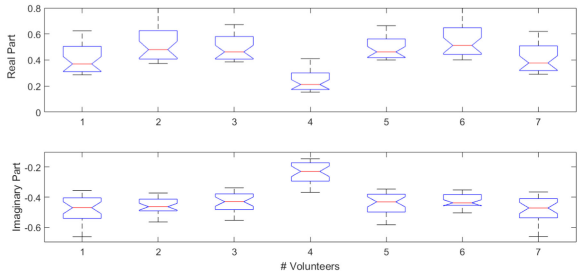

Fig. 10. Boxplot analysis of the absolute values of the frequency response complex impedance in all individuals in study case 1, first measurement, second nociceptor stimulation (P2).

a large BMI and thus the dispersion of liquid in the body may influence his values with respect to the others. Still, a variation is observed, in what the second nociceptor stimulation has slightly lower values of impedance. This could be attributed to the so called *memory* effect of the biological tissue.

Also an analysis on the sum of absolute values of the frequency response complex impedance in terms of boxplot representation has been performed. Figure 9 depicts the result for the time interval of first nociceptor stimulation, study case 1. Figure 10 depicts the result for the time interval of second nociceptor stimulation, study case 2.

F. Discussion

It is important to understand that the method and models developed here are uniquely defined for each individual. In other words, the reporting of the model values is not relevant here because the data is expressed with respect to the initial moment of measurement, whereas the state of the patient is taken as a reference. Hence, all values reported are in fact calibrated for that reference value of impedance and thus each individual has its own initial state values.

The use of FOIMs is now justified by the data in some sense that indeed, tissue memory exists and it is a feature naturally explained with properties of mathematical models from fractional calculus. The detailed description of properties of FOIMS has been given in numerous other reports, hence it is omitted here [41], [45].

The relevance of the data is nevertheless important, for it brings a method, device and mathematical models to provide an indication of change in bioelectrical impedance measured via skin electrodes correlated with absence/presence of nociceptor stimulation. This is then a first step towards developing a full objective measurement setup and algorithm for quantifying related pain levels.

Our proposed tools are in the same line of thought as those presented in [54], [55]. An intelligent analysis system based on fuzzy logic models was successfully tested in post-operative patients, whereas patient-controlled analgesia (Morphine based) was titrated from the determined index. With respect to their work, our work differs in that it delivers a mathematical framework related to the actual tissue dynamics (i.e., memory, dielectric) properties and thus justifies the use of FOIMs.

G. Limitations

The present study is limited in the number of individuals measured. Also, no chronic pain patients or ICU post-operatory pain patients have been included. The missing correlation to clinical practice indexes such as Wong-Baker faces scale or other numerical scores, should be performed on a larger population in order to extract a mathematical relationship between model parameters and clinical levels of pain.

Although the method is personalised, i.e., the values are calibrated to the initial state of the individual/patient, an analysis of the influence of BMI on the accuracy of the estimators should be performed.

The authors do not claim the values given here are reference values. They are specific for the individuals included in this study and calibrated for each individual in part.

The further development of these models can be the correlation to numerical scores for pain levels and self-feedback for determining a pain level index.

IV. Conclusion

In this work we provide a methodology and mathematical framework to model the nociceptor stimulation effect in healthy aware and awake individuals. The method used is bioelectrical impedance by means of non-invasive skin electrode measurement. The models proposed are physiologically based without direct correlation to the physiologicval quantities, i.e., they are calibrated for initial state of the individual. This implies a personalised assessment of nociceptor stimulation ef-

fect perceived as pain, hence unique parameterization of model values.

APPENDIX A
ON FRACTIONAL ORDER MODELS

The fractional calculus is a generalization of integration and derivation to non-integer (fractional) order operators. At first, we generalize the differential and integral operators into one fundamental operator D_t^n (n the order of the operation) which is known as *fractional calculus*.

Several definitions of this operator have been proposed (see, e.g., [45]). All of them generalize the standard differential–integral operator in two main groups: (a) they become the standard differential–integral operator of any order when n is an integer; (b) the Laplace transform of the operator D_t^n is s^n (provided zero initial conditions), and hence the frequency characteristic of this operator is $(j\omega)^n$.

A fundamental D_t^n operator, a generalization of integral and differential operators (*differ-integration* operator), is introduced as follows:

$$D_t^n = \begin{cases} \dfrac{d^n}{dt^n}, & n > 0 \\ 1, & n = 0 \\ \int_0^t (d\tau)^{-n}, & n < 0 \end{cases} \tag{6}$$

where n is the fractional order and $d\tau$ is a derivative function. Since the entire thesis will focus on the frequency-domain approach for fractional order derivatives and integrals, we shall not introduce the complex mathematics for time domain analysis. The Laplace transform for integral and derivative order n are, respectively:

$$L\left\{D_t^{-n} f(t)\right\} = s^{-n} F(s) \tag{7}$$

$$L\left\{D_t^{n} f(t)\right\} = s^{n} F(s) \tag{8}$$

where $F(s) = L\{f(t)\}$ and s is the Laplace complex variable. The Fourier transform can be obtained by replacing s by $j\omega$ in the Laplace transform and the equivalent frequency-domain expressions are:

$$\frac{1}{(j\omega)^n} = \frac{1}{\omega^n}\left(\cos\frac{\pi}{2} + j\sin\frac{\pi}{2}\right)^{-n} = \frac{1}{\omega^n}\left(\cos\frac{n\pi}{2} - j\sin\frac{n\pi}{2}\right) \tag{9}$$

$$(j\omega)^n = \omega^n\left(\cos\frac{\pi}{2} + j\sin\frac{\pi}{2}\right)^{n} = \omega^n\left(\cos\frac{n\pi}{2} + j\sin\frac{n\pi}{2}\right) \tag{10}$$

Thus, the modulus and the argument of the FO terms are given by:

$$Modulus(dB) = 20\log\left|(j\omega)^{\mp n}\right| = \mp 20n\log|\omega| \tag{11}$$

$$Phase(rad) = arg\left((j\omega)^{\mp n}\right) = \mp n\frac{\pi}{2} \tag{12}$$

resulting in:

- a Nyquist contour of a line with a slope $\mp n\frac{\pi}{2}$, anticlockwise rotation of the modulus in the complex plain around the origin according to variation of the FO value n;
- Magnitude (dB *vs* log-frequency): straight line with a slope of $\mp 20n$ passing through 0dB for $\omega = 1$;
- Phase (rad vs log-frequency): horizontal line, thus independent with frequency, with value $\mp n\frac{\pi}{2}$.

The respective sketches can be seen in Figure 11.

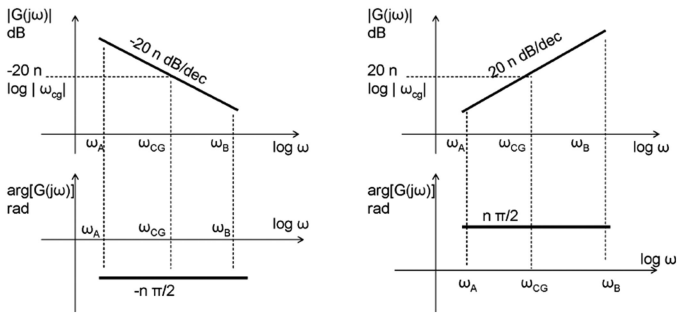

Fig. 11. Sketch representation of the FO integral and derivator operators in frequency domain, by means of the Bode plots (Magnitude, Phase).

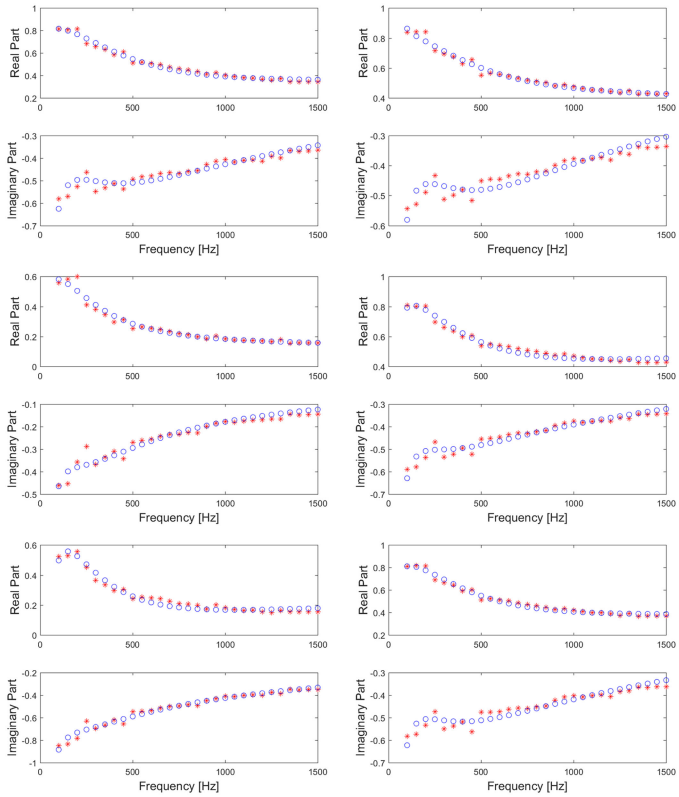

Fig. 12. Identification results for the transfer function model in remaining individuals: 'o' denotes model fitting and 'x' denotes experimental data.

APPENDIX B
IDENTIFICATION RESULTS FOR THE OTHER INDIVIDUALS

The results in the remaining 6 individuals for the transfer function model parameter identification are given here in Figure 12. The results are from the first pain stimuli, study case 1. Similar results are obtained for the other measurements as well.

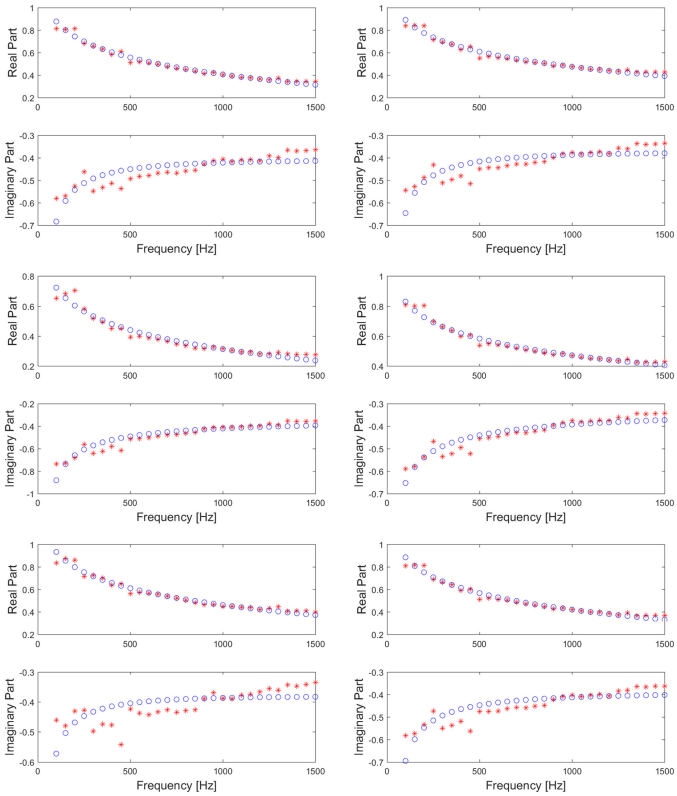

Fig. 13. Identification results for the FOIM model in remaining individuals: 'o' denotes model fitting and 'x' denotes experimental data.

The results in the remaining 6 individuals for the FOIM parameter identification are given here in Figure 13. The results are from the first pain stimuli, study case 1. Similar results are obtained for the other measurements as well.

Acknowledgment

The authors thank J. Juchem (Ghent University, Belgium) and Dr. L. Merrigo (University of Brescia, Italy) for their useful technical support during the development of the prototype device ANSPEC-PRO. The authors would like to thank M. Neckebroeck from Ghent University Hospital, Department of Anesthesia, Belgium, for the useful discussions on pain assessment and management.

Conflict of Interest: There are no conflicts of interest.

References

[1] R. Melzack, "From the gate to the neuromatrix," *Pain*, vol. 82, pp. S121–S126, 1999.
[2] P. Wall and R. Melzack, *The Challenge of Pain*. London, U.K: Penguin, 1996.
[3] E. Flaherty, "Using pain-rating scales with older adults," *Amer. J. Nursing*, vol. 108, no. 6, pp. 40–47, 2008.
[4] United States. Agency for Health Care Policy and Research and United States. Acute Pain Management Guideline Panel, Acute Pain Management: Operative or Medical Procedures and Trauma, U.S. Department of Health and Human Services, Public Health Service, Agency for Health Care Policy and Research, Acute Pain Management Guideline Panel, Washington DC, 1992.
[5] B. Gholami *et al.*, "Relevance vector machine learning for neonate pain intensity assessment using digital imaging," *IEEE Trans. Biomed. Eng.*, vol. 57, no. 6, pp. 1457–1466, Jun. 2010.
[6] J. Jacobi *et al.*, "Clinical practice guidelines for the sustained use of sedatives and analgesics in the critically ill adult," *Crit. Care Med.*, vol. 30, no. 1, pp. 119–141, 2002.
[7] K. Herr *et al.*, "Pain assessment in the non-verbal patient: Position statement with clinical practice recommendations," *Pain Manage. Nursing*, vol. 7, no. 2, pp. 44–52, 2006.
[8] T. Hadjistavropoulos *et al.*, "Using facial expressions to assess musculoskeletal pain in older persons," *Eur. J. Pain*, vol. 6, no. 3, pp. 179–187, 2002.
[9] W. M. Haddad *et al.*, "Neural network adaptive output feedback control for intensive care unit sedation and intraoperative anesthesia," *IEEE Trans. Neural Netw.*, vol. 18, no. 4, pp. 1049–1066, Jul. 2007.
[10] R. Hamill-Ruth and M. Marohn, "Evaluation of pain in the critically Ill patient," *Crit. Care Clinics*, vol. 15, no. 1, pp. 35–54, 1999.
[11] K. Puntillo *et al.*, "Use of a pain assessment and intervention notation (P.A.I.N.) tool in critical care nursing practice: Nurses' evaluations," *Heart Lung, J. Crit. Care*, vol. 31, no. 4, pp. 303–314, 2002.
[12] K. Puntillo *et al.*, "Relationship between behavioral and physiological indicators of pain," *Crit. Care Patients' Self-Rep. Pain Opoid Admin. Crit. Care Med.*, vol. 25, no. 7, pp. 1159–1166, 1997.
[13] N. Desbiens *et al.*, "Pain and satisfaction with pain control in seriously ill hospitalized adults: Findings from the SUPPORT research investigations. For the SUPPORT investigators. Study to understand prognoses and preferences for outcomes and risks of treatment," *Critical Care Medicine*, vol. 24, no. 12, pp. 1953–1961, 1996.
[14] P. McArdle, "Intravenous analgesia," *Crit. Care Clinics*, vol. 15, no. 1, pp. 89–104, 1999.
[15] C. Sessler *et al.*, "Multidisciplinary management of sedation and analgesia in critical care," *Seminars Respiratory Crit. Care Med.*, vol. 22, pp. 211–225, 2001.
[16] J. Kress and J. Hall, "Sedation in the mechanically ventilated patient," *Crit. Care Med.*, vol. 22, pp. 2541–2546, 2006.
[17] D. Copot *et al.*, "Data-driven modelling of drug tissue trapping using anomalous kinetics," *Chaos Solitons Fractals*, vol. 102, pp. 441–446, 2017.
[18] D. Copot *et al.*, "A systematic review of pain assessment in communicative and non-communicative patients," submitted for publication.
[19] V. Vijayakumar *et al.*, "Quantifying and characterizing tonic thermal pain across subjects from EEG data using random forest models," *IEEE Trans. Biomed. Eng.*, vol. 64, no. 12, pp. 2988–2996, Dec. 2017.
[20] L. J. Hadjileontiadis, "EEG-based tonic cold pain characterization using wavelet higher order spectral features," *IEEE Trans. Biomed. Eng.*, vol. 62, no. 8, pp. 1981–1991, Aug. 2015.
[21] C. M. Ionescu *et al.*, "Modeling of the lung impedance using a fractional order ladder network with constant phase elements," *IEEE Trans. Biomed. Eng.*, vol. 5, no. 1, pp. 83–89, Feb. 2011.
[22] J. Schuttler and H. Schwilden, *Modern Anesthetics.* Berlin, Heidelberg: Springer, 2008.
[23] C. Tsantoulas and X. McMahon, "Opening paths to novel analgesics: The role of potassium channels in chronic pain," *Trends Neurosci.*, vol. 37, no. 3, pp. 146–158, 2014.
[24] M. Liu and J. N. Wood, "The roles of sodium channels in nociception: Implications for mechanisms of neuropathic pain," *Pain Med.*, vol. 12, no. 3, pp. S93–S99, 2011.
[25] E. Sykova, "Extracellular potassium accumulation in the central nervous system," *Prog. Biophys. Mol. Biol.*, vol. 42, pp. 135–189, 1983.
[26] S. McMahon *et al.*, *Wall and Melzack's Textbook of Pain.* Philadelphia, PA, USA: Elsevier Saunders, 2013.
[27] D. Copot *et al.*, "Identification and performance analysis of fractional order impedance model for various test solutions," *in Proc. Int Conf. Fractional Differentiation Appl.*, NoviSad, Serbia, 2016, 542–550.
[28] Y. Yang *et al.*, "Multi-frequency simultaneous measurement of bioimpedance spectroscopy based on low crest factor multisine excitation," *Physiol. Meas.*, vol. 36, no. 3, pp. 489–501, 2015.
[29] R. Fish and L. Geddes, "Conduction of electrical current to and through the human body: A review," *ePlasty*, vol. 9, pp. 407–421, 2009.
[30] R. Pintelon and J. Schoukens, *System Identification: A Frequency Domain Approach.* Hoboken, NJ, USA: Wiley, 2001.
[31] CS Poon and T. Choy, "Frequency dispersions of human skin dielectrics," *Biophys. J.*, vol. 34, pp. 135–147, 1981.
[32] C. Gabriel *et al.*, "The dielectric properties of biological tissues: I. Literature survey," *Phys. Med. Biol.*, vol. 41, pp. 2231–2249, 1996.

[33] J. L. Vargas Luna *et al.*, "Dynamic impedance model of the skin-electrode interface for transcutaneous electrical stimulation," *PLoS One*, vol. 10, no. 5, 2015, Art. no. e0125609.
[34] I. Roeggen *et al.*, "Skin conductance variability between and within hospitalised infants at rest," *Early Hum. Develop.*, vol. 87, no. 1, pp. 37–42, 2011.
[35] K. E. Hagbarth *et al.*, "General characteristics of sympathetic activity in human skin nerves," *Acta Physiologica Scandinavica*, vol. 84, no. 2, pp. 164–176, 1972.
[36] G. F. Goddard, "A pilot study of the changes of skin electrical conductance in patients undergoing general anaesthesia and surgery," *Anaesthesia*, vol. 37, no. 4, pp. 408–415, 1982.
[37] C. M. Ionescu *et al.*, "The role of fractional calculus in modelling biological phenomena: A review," *Commun. Nonlinear Sci. Numer. Simul.*, vol. 51, pp. 141–159, 2017.
[38] C. M. Ionescu, "The phase constancy in neural dynamics," *IEEE Trans. Syst. Man Cybern., A Syst. Humans*, vol. 42, no. 6, pp. 1543–1551, Nov. 2012.
[39] R. Bogacz, "A tutorial on the free-energy framework for modelling perception and learning," *J. Math. Psychol.*, vol. 76, pp. 198–211, 2017.
[40] G. Tononi, "An information integration theory of consciousness," *BMC Neurosci.*, vol. 5, p. 42, 2004.
[41] R. Magin, "Fractional calculus in bioengineering," *Crit. Rev. Biomed. Eng.*, vol. 32, no. 1, pp. 1–104, 2004.
[42] B. West, "Fractal physiology and the fractional calculus: A perspective," *Frontiers Physiol.*, vol. 1, pp. 1–12, 2010, doi: 10.3389/fphys.2010.00012.
[43] X. J. Zhou *et al.*, "Studies of anomalous diffusion in the human brain using fractional order calculus," *Magn. Reson. Med.*, vol. 63, no. 3, pp. 562–569, 2010.
[44] C. Nicholson, "Diffusion and related transport properties in brain tissue," *Rep. Prog. Phys.*, vol. 64, pp. 815–884, 2001.
[45] I. Podlubny, "Geometric and physical interpretation of fractional integration and fractional differentiation," *Fractional Calculus Appl. Anal.*, vol. 5, no. 4, pp. 367–386, 2002.
[46] Y. Li *et al.*, "MittagLeffler stability of fractional order nonlinear dynamic systems," *Automatica*, vol. 45, no. 8, pp. 1965–1969, 2009.
[47] Y. Li *et al.*, "Stability of fractional-order nonlinear dynamic systems: Lyapunov direct method and generalized MittagLeffler stability," *Comput. Math. Appl.*, vol. 59, no. 5, pp. 1810–1821, 2010.
[48] C. M. Ionescu, "A memory-based model for blood viscozity," *Commun. Nonlinear Sci. Numer. Simul.*, vol. 45, pp. 29–34, 2017.
[49] J. Trujillo, "Fractional models: Sub and super-diffusives, and undifferentiable solutions," *Innov. Eng. Comput. Technol.*, pp. 371–401, 2006.
[50] D. Wheatley, "Diffusion theory, the cell and the synapse," *Biosystems*, vol. 45, pp. 151–163, 1998.
[51] B. Lundstrom *et al.*, "Fractional differentiation by neocortical pyramidal neurons," *Nature Neurosci.*, vol. 11, pp. 1335–1342, 2008.
[52] D. Sierociuk *et al.*, "Diffusion process modeling by using fractional-order models," *Appl. Math. Comput.*, vol. 257, pp. 2–11, 2015.
[53] N. D. Crosby *et al.*, "Burst and tonic spinal cord stimulation differentially activate GABAergic mechanisms to attenuate pain in a rat model of cervical radiculopathy," *IEEE Trans. Biomed. Eng.*, vol. 62, no. 6, pp. 1604–1613, Jun. 2015.
[54] J. S. Shieh *et al.*, "A novel fuzzy pain demand index derived from patient-controlled analgesia for postoperative pain," *IEEE Trans. Biomed. Eng.*, vol. 54, no. 12, pp. 2123–2132, Dec. 2007.
[55] J. S. Shieh *et al.*, "Comparison of the applicability of rule-based and self-organizing fuzzy logic controllers for sedation control of intracranial pressure pattern in a neurosurgical intensive care unit," *IEEE Trans. Biomed. Eng.*, vol. 53, no. 8, pp. 1700–1705, Aug. 2006.